

Increasing quantum yield of sodium salicylate above 80 eV photon energy: Implications for photoemission cross sections

D. W. Lindle, T. A. Ferrett, P. A. Heimann, and D. A. Shirley

*Materials and Molecular Research Division, Lawrence Berkeley Laboratory, Berkeley, California 94720
and Department of Chemistry, University of California, Berkeley, California 94720*

(Received 21 November 1985)

The quantum yield of the visible scintillator sodium salicylate is found to increase in the incident photon-energy range 80–270 eV. Because of its use as a photon-flux monitor in recent gas-phase photoelectron spectroscopy measurements, previously reported partial cross sections for Hg (*4f*, *5p*, and *5d* subshells) and CH₃I (I *4d* subshell) in this energy range are corrected, and new values are reported. For Hg, the correction brings the experimental data into better overall agreement with theory. However, considerable uncertainty remains in the absolute scale derived from previous Hg photoabsorption measurements, and no single rescaling of the subshell cross sections could simultaneously bring all three into agreement with available theoretical calculations.

I. INTRODUCTION

The determination of photoemission cross sections using synchrotron radiation in the photon-energy range in which core-level electrons can be ionized (~50 eV and higher) requires a reliable photon-flux monitor. For our measurements, we chose the visible scintillator sodium salicylate, because it was reported to have a constant quantum yield of optical photons relative to incident photons to within 5%, for incident photon energies up to 107 eV.¹ Based on the assumption that this quantum yield remains constant at higher photon energies, we recently reported partial cross-section results up to 270 eV for the Hg *4f*, *5p*, and *5d* subshells,² and the methyl iodide I *4d* subshell.³

The measurements of Hg photoemission cross sections² indicated the existence of a large apparent discrepancy with theoretical calculations^{4–8} for the *4f* partial cross section, and lesser differences for the *5p* and *5d* cross sections. These findings were especially puzzling for the *4f* subshell because of the concurrence of several theories,^{6–8} and because it was expected that the calculations for the dominant *4f* photoemission channel would not be complicated by large interchannel interactions.⁸ In addition, the same calculations predicted the angular distribution of Hg *4f* photoelectrons quite well. For these reasons, we became suspicious that a significant systematic error was present in our cross-section measurements, with the unknown high-photon-energy quantum yield of sodium salicylate being a plausible candidate.

We report here a measurement of a significant increase in the quantum yield of the visible scintillator sodium salicylate in the photon-energy range 80–270 eV; approximately a factor of 2 under our experimental conditions. The measured increase in the relative quantum yield was determined from a comparison to the known energy dependence of the Ne *2p* photoemission cross section.⁹ Similar measurements indicating the same qualitative increase for the quantum yield of sodium salicylate have

been obtained independently in two other laboratories.^{10,11} Using the newly measured quantum yield, we correct the previously reported cross sections for Hg and CH₃I.

Because the quantum-yield determination was made in the context of searching for a possible systematic error, Sec. II contains a description of the search which culminated in the measured variation in the relative quantum yield of sodium salicylate. Section III describes the corrections to the earlier photoemission data.

II. THE QUANTUM YIELD

The earlier photoelectron spectroscopy (PES) measurements^{2,3} were made with an angle-resolved time-of-flight (TOF) apparatus¹² using synchrotron radiation from beam line III-1 at the Stanford Synchrotron Radiation Laboratory (SSRL). To determine relative partial cross sections, one TOF analyzer placed at 54.7° with respect to the photon polarization measures photoemission peak intensities $I(h\nu)$ as a function of photon energy. The dependence of these intensities on experimental quantities in the dipole approximation¹³ is given by

$$I(h\nu) \propto T(\epsilon)p\sigma(h\nu)N(h\nu), \quad (1)$$

where $T(\epsilon)$ is the relative transmission of the TOF analyzer as a function of electron kinetic energy ϵ , p is the gas sample pressure, $\sigma(h\nu)$ is the energy-dependent partial cross section, and $N(h\nu)$ is the relative photon flux when the monochromator energy is set at $h\nu$.

To determine unknown cross sections, knowledge of the analyzer transmission $T(\epsilon)$ is required. Qualitatively, the kinetic energy dependence of $T(\epsilon)$ for a TOF analyzer is governed by two effects. First, in the free-flight path from the interaction region to the channel-plate detector, the photoelectrons are influenced by residual stray magnetic fields and built-up electric charges, with the lowest-energy electrons being discriminated against. Second, after leaving the free-flight region, the electrons are accelerated by 100 V before impacting a channel-plate detec-

tor. It is known¹⁴ that the channel-plate response is essentially constant throughout the electron-energy range applicable to this work. Considering these two contributions, $T(\epsilon)$ should increase monotonically with ϵ , reaching an asymptotic value at high ϵ . This behavior reflects the relative simplicity of the TOF technique for electron-energy analysis. Previous observations have indicated that for all practical purposes $T(\epsilon)$ reaches a constant asymptotic value at kinetic energies greater than 20 eV.

Quantitatively, determination of $T(\epsilon)$ for the 54.7° TOF detector is accomplished by measuring photoelectron peak intensities as a function of kinetic energy for subshells with known partial cross sections, such as Ne 2*p* and 2*s*,⁹ while simultaneously measuring the sample pressure and monitoring the photon flux with the scintillator sodium salicylate. Figure 1 shows a $T(\epsilon)$ curve measured for high-kinetic-energy Ne 2*p* photoelectrons (binding energy is 21.6 eV), plotted as a function of photon energy in the range 80–270 eV. The results in Fig. 1 were determined assuming a constant quantum yield for sodium salicylate. As noted above, at such high kinetic energies we expect the relative transmission $T(\epsilon)$ of our analyzer to be constant. To investigate the measured decrease of $T(\epsilon)$ by a factor of 2, we start by rewriting Eq. (1):

$$T(\epsilon) \propto \frac{I(h\nu)}{p\sigma(h\nu)N(h\nu)}. \quad (2)$$

Assuming that $T(\epsilon)$ should be constant at high kinetic energy ($\epsilon > 58$ eV in Fig. 1), we will examine each factor on the right-hand side of Eq. (2) to determine which one is responsible for the measured decrease in $T(\epsilon)$. For the measured peak intensity $I(h\nu)$, we consider only those effects independent of the pressure, partial cross section, and photon flux, because those parameters are examined separately. As we shall see, our examination of Eq. (2) will lead us to the conclusion that an increase in the quantum yield of sodium salicylate is the most likely cause of the deviation of $T(\epsilon)$ from constancy displayed in Fig. 1.

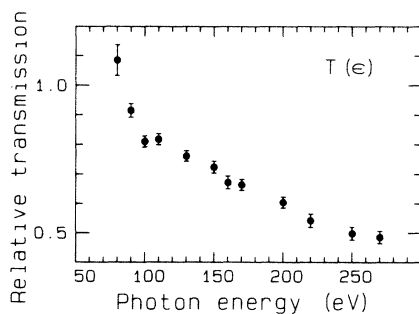


FIG. 1. Relative transmission function $T(\epsilon)$ for the 54.7° TOF analyzer determined with Ne 2*p* photoelectrons shown as a function of photon energy, after correction for second-order contributions to the synchrotron-radiation flux as described in the Appendix, and assuming a constant quantum yield for sodium salicylate. The Ne 2*p* binding energy is 21.6 eV, so that the lowest kinetic energy represented is approximately 58 eV. The average of the two lowest-energy points has been normalized to unity.

A major breakdown of the dipole approximation could lead to variations in $I(h\nu)$ measured at 54.7° with increasing photon energy, as the nondipole effects become increasingly more important. However, this possibility can be ruled out on several counts. Experimentally, no evidence for nondipole effects in the Ne 2*p* subshell has been observed in the 100–150-eV photon-energy range, and only small manifestations of such effects were seen at the much higher photon energies of 1254 and 1487 eV.¹⁵ Theoretically, only very small nondipole effects are expected for low-*Z* elements in the photon and photoelectron energy ranges pertinent to Fig. 1.¹⁶ Furthermore, the measured Ne cross sections and angular distributions⁹ are predicted well by theoretical calculations which assume the dipole approximation.¹⁷

Another factor that could induce changes in $I(h\nu)$ would be a strongly energy-dependent photon polarization. However, the magnitude of the change in $T(\epsilon)$ shown in Fig. 1 would require a reversal of the synchrotron radiation linear polarization from horizontal to vertical in the 80–270-eV photon-energy range. Although the photon polarization has not been measured systematically for monochromators at SSRL, a large body of angular-distribution measurements made on beam line III-1 is inconsistent with anything but a high degree of horizontal linear polarization in this energy range. In addition, the well-understood properties of synchrotron radiation¹⁸ argue strongly against a substantial variation in polarization.

Finally, we considered the possibility that some photon-beam movement as a function of photon energy caused the TOF analyzer to “see” fewer electrons in its aperture-defined viewing region, while the photon-flux monitor, with a larger viewing area, saw no apparent change. We dismiss this explanation, however, because the simultaneous measurement of the ratio of transmissions $T(\epsilon)$ of two TOF analyzers at 0° and 54.7° (determined¹² with the known Ne 2*p* angular distribution⁹) was constant to within 2% over the same photon-energy range. The relative efficiency is as sensitive to changes in the experimental geometry as the transmission function $T(\epsilon)$ for the 54.7° analyzer. This observation for the efficiency provides an additional argument against the possibility of changing photon polarization.

The Ne pressure p , monitored behind the nozzle which allows gas into the interaction region, was measured with a capacitance manometer to an estimated accuracy of $\pm 2\%$. While it is possible that the relationship between the measured pressure and the sample density in the interaction region is nonlinear, this possibility can be eliminated because the flow of Ne was uninterrupted and steady for the results in Fig. 1. Furthermore, to guard against systematic changes, the points at different photon energies in Fig. 1 were obtained in a random order and repeated at random.

Moving on to the Ne 2*p* cross section $\sigma(h\nu)$, the literature values are accurate to $\pm 8\%$ or better over the entire energy range studied.⁹ In addition, the values are based on several independent determinations and compilations of the absolute total cross section of Ne.⁹

A determination of the photon flux $N(h\nu)$ for use in

obtaining $T(\varepsilon)$ from Eq. (2) is predicated on the assumption that all of the photons in the synchrotron-radiation beam are of energy $h\nu$. In general, higher-order (e.g., $2h\nu$) and scattered (all energies) photons also are present, and will add to the apparent $N(h\nu)$ with no concomitant increase in the measured peak intensity $I(h\nu)$. Because higher-order contamination commonly provides the largest experimental uncertainty in intensity measurements using synchrotron radiation, small contributions from second-order radiation, detected by photoemission, have been corrected for carefully by the procedure described in the Appendix. No photoemission induced by orders higher than second was observed in the TOF spectra. A large contribution from scattered light is inconsistent both with the very low background in our photoelectron spectra and with measurements of the total photon flux in the vicinity of the carbon K edge.¹⁹ We estimate that scattered photons contribute at most 10%, and probably much less, to the total photon flux between 80 and 270 eV. No corrections for scattered-light intensity were made.

Determination of the relative synchrotron-radiation flux $N(h\nu)$ is accomplished by measuring the photocurrent from a photomultiplier tube (RCA 8850) which is sensitive to the visible fluorescence emitted by sodium salicylate after illumination by vacuum-ultraviolet photons. The quantum yield of sodium salicylate $Q(h\nu)$, from 50 to 107 eV photon energy has been reported to be constant to within 5%,¹ and we have assumed in earlier experiments^{2,3} that it remains so up to the carbon K edge near 280 eV. However, an increase in $Q(h\nu)$ at higher energies is expected because the quantum yield determined with x-rays²⁰ is much larger than $Q(h\nu)$ below 107 eV.¹ An increase in $Q(h\nu)$ could explain the behavior exhibited in Fig. 1, because the measured analyzer transmission $T(\varepsilon)$ and the relative photon flux $N(h\nu)$ are inversely related [see Eq. (2)], and because our measurements of $N(h\nu)$ are directly proportional to $Q(h\nu)$. Other photon-flux variations are mitigated by the random data collection mentioned above. We note that variations in the photon flux due to the storage ring source and monochromator are properly accounted for in our normalization procedure.

Having exhausted other reasonable possibilities, we conclude that the changing quantum yield of sodium salicylate is the major cause of the decrease in the measured $T(\varepsilon)$ displayed in Fig. 1. Accordingly, we show in Fig. 2 the relative quantum yield of sodium salicylate, $Q(h\nu)$, assuming the transmission of the TOF analyzer $T(\varepsilon)$ is constant. The relative values of $Q(h\nu)$ in Fig. 2 were simply taken as the inverse of the measurements in Fig. 1. The qualitative increase exhibited in $Q(h\nu)$ in this energy range recently has been corroborated by Nordgren and Nyholm,¹⁰ and by Samson,¹¹ although our observation of an increase in $Q(h\nu)$ at energies as low as 80 eV may be in conflict with earlier measurements.¹

We expect that measurements of the sodium salicylate quantum yield from different laboratories may vary because of differences in experimental parameters. For example, differences in the higher-order and scattered-light contributions to the incident radiation could affect the measured quantum yield significantly. Another potential

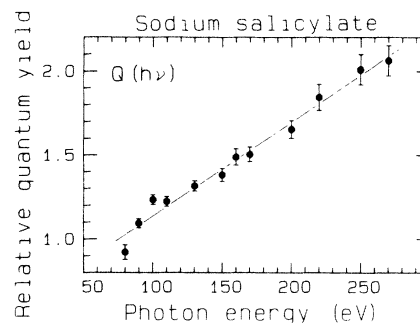


FIG. 2. Relative quantum yield of sodium salicylate $Q(h\nu)$ vs photon energy, taken as the inverse of the results in Fig. 1, assuming the 54.7° TOF analyzer transmission is constant at high kinetic energies. The line is a linear least-squares fit to the data, described by $Q(h\nu) = 0.576 + 0.0056(2)h\nu$, for $80 \leq h\nu \leq 270$ and with $h\nu$ expressed in eV.

difference between experiments may result from the techniques used to normalize to the incident photon flux. In the present work, we used Ne $2p$ photoemission, whereas other measurements used either Au total electron yields,¹⁰ or Ne total ion yields.¹¹ Finally, the methods used to detect the visible fluorescence from sodium salicylate are different for all three measurements,^{10,11} meaning that variations in scintillator thickness, experimental geometry, or possibly the spectral distribution of the fluorescence as a function of incident photon energy may all be important to the quantitative results. As a result of these many unknowns, we report only the *qualitative* observation that the quantum yield of sodium salicylate increases in the 80–270-eV photon-energy range. We consider the factor-of-2 increase to be quantitatively correct for our ex-

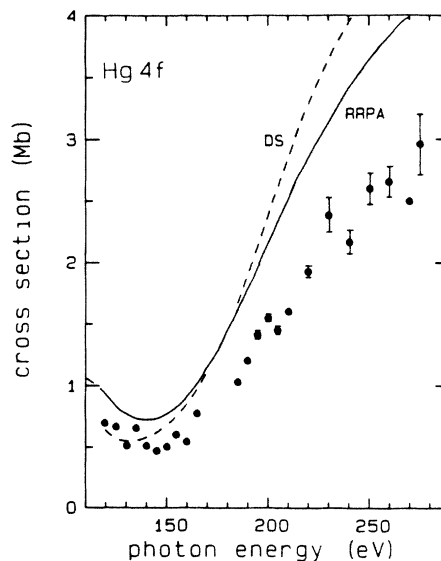


FIG. 3. Hg $4f$ cross section (Ref. 2) after correction for the changing quantum yield of sodium salicylate. The solid and dashed curves are RRPA (Ref. 7) and DS (Ref. 8) calculations, respectively.

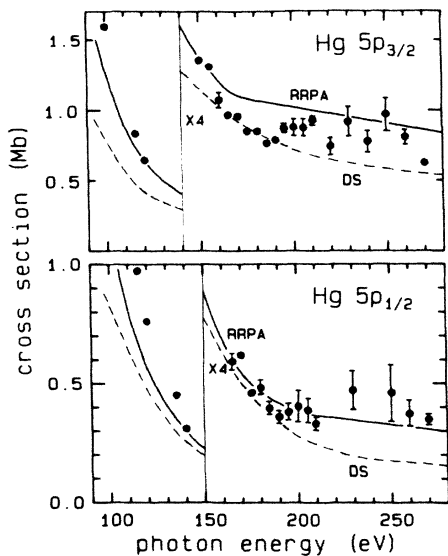


FIG. 4. Hg $5p_{3/2}$ and $5p_{1/2}$ cross sections as in Fig. 3.

perimental conditions, but appropriate caution should be used in applying the present results to other laboratories, especially in light of the larger increases with photon energy measured by other workers.^{10,11}

III. IMPLICATIONS FOR PHOTOEMISSION CROSS SECTIONS

The consequences of this measurement of $Q(h\nu)$ for our cross-section results in this photon-energy range are obvious. Two previous studies yielded cross sections in this range for atomic Hg (Ref. 2) and CH_3I .³ We have corrected these data for the $Q(h\nu)$ shown in Fig. 2, and the new results are shown in Figs. 3–6. We briefly discuss the implications of the new cross-section values.

The corrected Hg $4f$ cross-section data appear in Fig. 3. The delayed onset of the $4f \rightarrow \epsilon g$ channel is more pronounced now, and the agreement with theory is much improved. However, the calculated curves are still higher than the experimental data by approximately 50%. Due to uncertainties in photoabsorption measurements,^{21,22} the absolute scale of the Hg photoemission data could be off

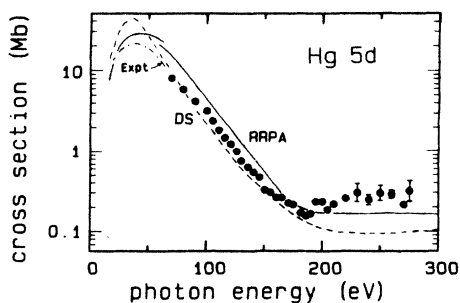


FIG. 5. Hg $5d$ cross section as in Fig. 3. Dashed-dotted curve is from absorption measurements (Refs. 21 and 22). The low-energy solid curve is also a RRP calculation (Ref. 25).

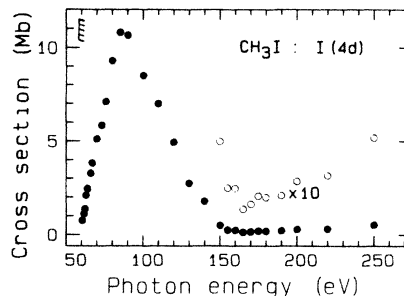


FIG. 6. CH_3I I $4d$ cross section (Ref. 3) after correction for the changing quantum yield of sodium salicylate.

by as much as 30%,² possibly explaining much of the discrepancy with theory. Regardless of any correction in the normalization of the $4f$ data, the overall shape of the experimental curve will remain the same. We note that a rescaling of the data in Fig. 3 could not bring them into agreement with the Dirac-Slater (DS) curve,⁸ whereas the relativistic random-phase approximation (RRPA) curve⁷ may be reconcilable with the $4f$ data in this way.

Another explanation²³ which could account for the remaining difference between theory and experiment for the $4f$ cross section has been suggested for the RRP calculations. Because the RRP equations include only single-ionization channels but require the calculated partial cross sections to sum to the correct integrated oscillator strength, it might be expected that the calculations will overestimate inner-shell cross sections for cases in which significant multielectron processes (i.e., double excitation and ionization) are occurring. No experimental data for Hg double excitation or ionization are available in this energy range to check this hypothesis.

Figures 4 and 5 show mixed changes in agreement with theory for $5p$ and $5d$ photoemission from Hg, respectively. The agreement for the $5p$ channels is very good, and the Cooper minima in these channels are now more apparent. However, the corrected $5d$ cross section deviates substantially from the theoretical curves at the highest energies; the $5d$ Cooper minimum shows up experimentally as a true cross-section minimum. Considering the set of Hg partial cross sections in Figs. 3–5, it is clear that no single renormalization of the data can reconcile the available theoretical calculations with our corrected results.

The I $4d$ cross section of CH_3I , shown in Fig. 6, exhibits an enhancement in the observed Cooper minimum after application of the correction for the sodium salicylate quantum yield. There are no theoretical calculations for this subshell available for comparison.

ACKNOWLEDGMENTS

We thank J. A. R. Samson, J. Nordgren, and R. Nyholm for helpful discussions and for making their results available prior to publication, and S. T. Manson for pointing out the importance of the Hg $4f$ cross-section discrepancy. This work was supported by the Director, Office of Energy Research, Office of Basic Energy Sciences, Chemical Sciences Division of the U. S. Department of Energy

under Contract No. DE-AC03-76SF00098. It was performed at the Stanford Synchrotron Radiation Laboratory, which is supported by the Department of Energy's Office of Basic Energy Sciences.

APPENDIX: CORRECTION OF THE RELATIVE TRANSMISSION FOR SECOND-ORDER-LIGHT CONTRIBUTIONS TO THE PHOTON FLUX

The values of $T_0(\epsilon)$ [$T_0(h\nu)$ (Ref. 24)] (a subscript zero denotes uncorrected values) determined from Eq. (2) without correcting for second-order-light contributions to $N_0(h\nu)$ (not shown) exhibit a similar qualitative trend with photon energy as shown by the corrected values of $T(h\nu)$ in Fig. 1, because the fraction of photons that are second order is relatively small ($\leq 15\%$) in this energy range. Quantitatively, the decrease with energy of $T_0(h\nu)$ is suppressed, necessitating the second-order correction described below.

The determination of the relative amount of second-order light is accomplished by comparison of the peak intensities, $I(h\nu)$ and $I(2h\nu)$, for Ne $2p$ photoemission induced by first- and second-order radiation in each TOF spectrum. The ratio of peak intensities [see Eq. (1)] measured when the monochromator is set at $h\nu$ is given by

$$\frac{I(2h\nu)}{I(h\nu)} = R(h\nu) \frac{\sigma(2h\nu)}{\sigma(h\nu)}, \quad (\text{A1})$$

where $R(h\nu)$ is the ratio of second- to first-order flux, $N(2h\nu)/N(h\nu)$. The values of $R(h\nu)$ derived from Eq. (A1) can be used to correct the measurement of the relative photon flux $N_0(h\nu)$, if care is taken to recognize that the first- and second-order contributions to $N_0(h\nu)$ are weighted differently, with relative weights equal to $Q(h\nu)$ and $Q(2h\nu)$, respectively.

The correction to $T_0(h\nu)$ due to second-order-light contributions to $N_0(h\nu)$ can be written [see Eq. (2)]

$$T(h\nu) = \frac{T_0(h\nu)N_0(h\nu)}{N(h\nu)} = T_0(h\nu)[1 + R(h\nu)\chi(h\nu)] \propto \frac{1}{Q(h\nu)}, \quad (\text{A2})$$

$$\chi(h\nu) = \frac{Q(2h\nu)}{Q(h\nu)} = \frac{T(h\nu)}{T(2h\nu)}, \quad (\text{A3})$$

where $\chi(h\nu)$ represents the relative weighting of the contributions to $N_0(h\nu)$ of photons of energy $2h\nu$ and $h\nu$. The following steps yield the corrected values $T(h\nu)$.

(1) For $h\nu=150$ and 160 eV, no second-order Ne $2p$ photoemission was discernible [i.e., $R(h\nu) \ll 1\%$], because the second-order energies of 300 and 320 eV were absorbed by a carbon window.¹⁹

(2) Combining Eqs. (A2) and (A3), solving for $T(h\nu)$, and using $T(160)$ from step (1) we find, for $h\nu=80$ eV,

$$T(80) = T_0(80)[1 - C(80)]^{-1}, \quad (\text{A4})$$

$$C(80) = \frac{T_0(80)R(80)}{T(160)}.$$

(3) For photon energies above 160 eV, we assume $1.5 \leq \chi(h\nu) \leq 2.5$, yielding $T(h\nu)$ for 170 – 270 eV using Eq. (A2). This large range of values for $\chi(h\nu)$ is consistent with measurements¹⁰ of $Q(h\nu)$ above 300 eV, and with the present results at lower energies, and introduces only small errors in the corrected $T(h\nu)$ because the amount of second-order light for $h\nu \geq 170$ eV is small (2 – 10%).

(4) Having determined the corrected values for $h\nu \geq 170$ eV in step (3), we use them in Eq. (A4) for $h\nu=90, 100, 110,$ and 130 eV.

The final results, corrected for second-order contributions as outlined above, are shown in Fig. 1.

¹J. A. R. Samson and G. N. Haddad, *J. Opt. Soc. Am.* **64**, 1346 (1974).

²P. H. Kobrin, P. A. Heimann, H. G. Kerkhoff, D. W. Lindle, C. M. Truesdale, T. A. Ferrett, U. Becker, and D. A. Shirley, *Phys. Rev. A* **27**, 3031 (1983).

³D. W. Lindle, P. H. Kobrin, C. M. Truesdale, T. A. Ferrett, P. A. Heimann, H. G. Kerkhoff, U. Becker, and D. A. Shirley, *Phys. Rev. A* **30**, 239 (1984).

⁴J. S. Shyu and S. T. Manson, *Phys. Rev. A* **11**, 166 (1975).

⁵F. Keller and F. Combet Farnoux, *J. Phys. B* **12**, 2821 (1979).

⁶F. Keller and F. Combet Farnoux, *J. Phys. B* **15**, 2657 (1982).

⁷W. R. Johnson and V. Radojević, *Phys. Lett.* **92A**, 75 (1982).

⁸B. R. Tambe and S. T. Manson, *Phys. Rev. A* **30**, 256 (1984).

⁹F. Wuilleumier and M. O. Krause, *J. Electron Spectrosc.* **15**, 15 (1979).

¹⁰J. Nordgren and R. Nyholm (private communication).

¹¹J. A. R. Samson (private communication).

¹²M. G. White, R. A. Rosenberg, G. Gabor, E. D. Poliakoff, G. Thornton, S. Southworth, and D. A. Shirley, *Rev. Sci. Instrum.* **50**, 1288 (1979); S. Southworth, C. M. Truesdale, P. H.

Kobrin, D. W. Lindle, W. D. Brewer, and D. A. Shirley, *J. Chem. Phys.* **76**, 143 (1982).

¹³C. N. Yang, *Phys. Rev.* **74**, 764 (1948).

¹⁴M. Galanti, R. Gott, and J. F. Renaud, *Rev. Sci. Instrum.* **42**, 1818 (1971); E. A. Kurz, *Am. Lab.*, March (1979).

¹⁵F. Wuilleumier and M. O. Krause, *Phys. Rev. A* **10**, 242 (1974).

¹⁶H. K. Tseng, R. H. Pratt, S. Yu, and A. Ron, *Phys. Rev. A* **17**, 1061 (1978).

¹⁷W. R. Johnson and K. T. Cheng, *Phys. Rev. A* **20**, 978 (1979), and references therein.

¹⁸H. Winick, in *Synchrotron Radiation Research*, edited by H. Winick and S. Doniach (Plenum, New York, 1980).

¹⁹The experimental apparatus was separated from the monochromator by a thin carbon window, which absorbs very strongly at the carbon K edge starting at ~ 280 eV. Because most of the total photon flux was absorbed by the window at this edge, it is clear that most of the photons were first order, rather than higher-order or scattered photons.

²⁰E. Krokowski, *Naturwiss.* **45**, 509 (1958).

²¹R. B. Cairns, H. Harrison, and R. I. Schoen, *J. Chem. Phys.* **53**, 96 (1970).

²²J. L. Dehmer and J. Berkowitz, *Phys. Rev. A* **10**, 484 (1974).

²³D. W. Lindle, P. A. Heimann, T. A. Ferrett, P. H. Kobrin, C. M. Truesdale, U. Becker, H. G. Kerkhoff, and D. A. Shirley, *Phys. Rev. A* **33**, 319 (1986).

²⁴We use the symbol $T(h\nu)$ in place of $T(\epsilon)$ for the relative

transmission because we are trying to determine $Q(h\nu)$, which produces a photon-energy-dependent effect on the relative transmission. For calibration with Ne $2p$ photoelectrons, $T(h\nu) = T(\epsilon + 21.6 \text{ eV})$.

²⁵W. R. Johnson, V. Radojević, P. Deshmukh, and K. T. Cheng, *Phys. Rev. A* **25**, 337 (1982).